Development and Operation of Large Centrifuge at PWRI

by

Osamu Matsuo[1], Tatsuya Tsutsumi[2], Mitsu Okamura[3], Tetsuya Sasaki[2] and Kunio Nishi[4]

ABSTRACT

A large geotechnical centrifuge with a radius of 6.6 m has been developed at Public Works Research Institute in 1997. For the purpose of the geotechnical earthquake studies, a powerful electro-hydrauric shaking table designed to work in the centrifuge has also been developed. This shaking table provides 40G shaking acceleration to a model of 1 ton, which acceleraton is equivalent to the maximum ground acceleration observed during the 1995 Hyogoken Nanbu earthquake for a model at 50G centrifugal acceleration field.

The centrifuge has been under extensive use to investigate various geotechnical problem. Results of centrifuge tests carried out so far are briefly described.

Key Words: Geotechnical Centrifuge, Shaking Table, Model test Retaining Wall

1. INTRODUCTION

Public Works Research Institute (PWRI) constructed first geotechnical centrifuge with a radius of 1.25 m in 1961. With increasing needs of geotechnical earthquake studies, the second centrifuge with a radius of 2.0 m was introduced in 1987 with a shaking table having a capacity of 4G·ton. This centrifuge has been used to study various boundary value problems including soil liquefaction, seismic slope stability, soil improvement techniques, tunnel excavation, and so on.

The Hyogoken Nanbu earthquake, January 17, 1995, that hit the densely populated area caused devastating damages to human lives and properties. It also demonstrated various earthquake geotechnical problems. Immediately after the quake, PWRI, the Ministry of Construction headquarters and the Government decided to construct a new centrifuge with a shaker which can simulate strong ground motion observed in the past earthquake. PWRI initiated basic and detailed design works in May, 1995. Construction of the centrifuge and the enclosure started in March, 1996 and completed in March, 1997.

In this paper, notable features of the centrifuge are described in detail and results of dynamic centrifuge tests on retaining walls are also discussed.

2. CENTRIFUGE SPECIFICATIONS

The centrifuge that has been newly installed at PWRI is the largest centrifuge in Japan, with a effective radius of 6.6m and maximum payload of 2.7 tons at up to 150G (400G · ton). A photograph and a schematic illustration of the centrifuge are shown in **Fig.1** and **2**, respectively. Notable specifications are summarized in **Table 1**. The main parts of the centrifuge are housed in an underground reinforced concrete pit, 17.0 m in diameter and 4.6 m deep. A pair of hydraulic jacks is installed at one side of rotation arm. When the platform swing up, these jacks push the swing platform to sit on the end plate of the arm so that strong earthquake motions can be simulated by fixing the swing platform to the rigid rotating arm. This is called "Touch-down System" (Nagura et al. 1994).

In order to eliminate the imbalance moment produced during spinning, a in-flight automatic balancing system is equipped. In-flight balancing is achieved by moving two balancing weights on the rotation arm. When the balance

1) Head, Soil dynamics division, Earthquake Disaster Prevention Research Center, Public Work Research Institute, Ministry of Construction, Tsukuba city 3050804, Japan
2) Research Engineer, ditto
3) Senior Research Engineer, ditto
4) Research Engineer, Technical Institute, Hazama Corporation, Tsukuba city, Japan

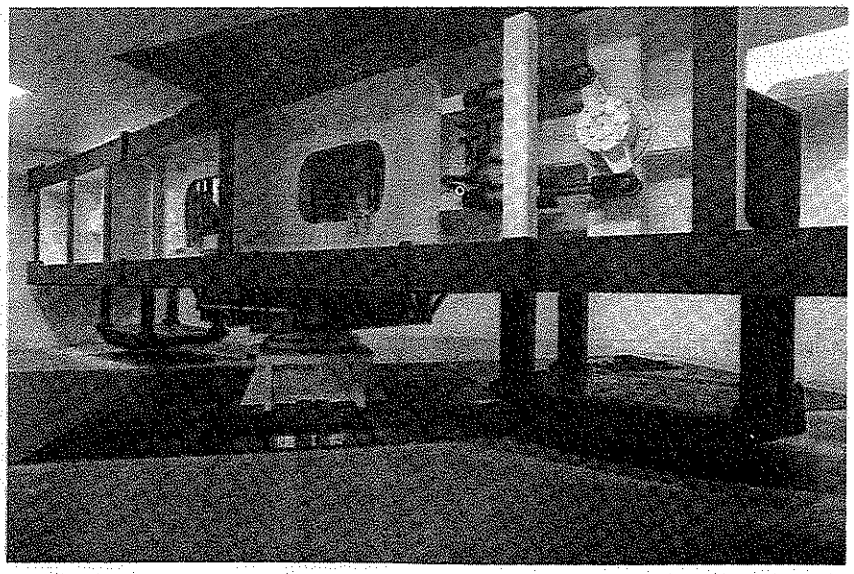

Fig.1 Photograph of the centrifuge

Table 1 Specification of centrifuge

Effective Rotor Radius	6.6 m
Maximum Acceleration	static test : 150 g dynamic test : 100 g
Payload Weight	5 ton
Payload Capacity	400 g-ton
Swing Platform	static test : 2 dynamic test : 1
Platform Space	length : 2.4 m width : 1.3 m height : 1.0 m
Data Acquisition	static test : 100 ch dynamic test : 80 ch

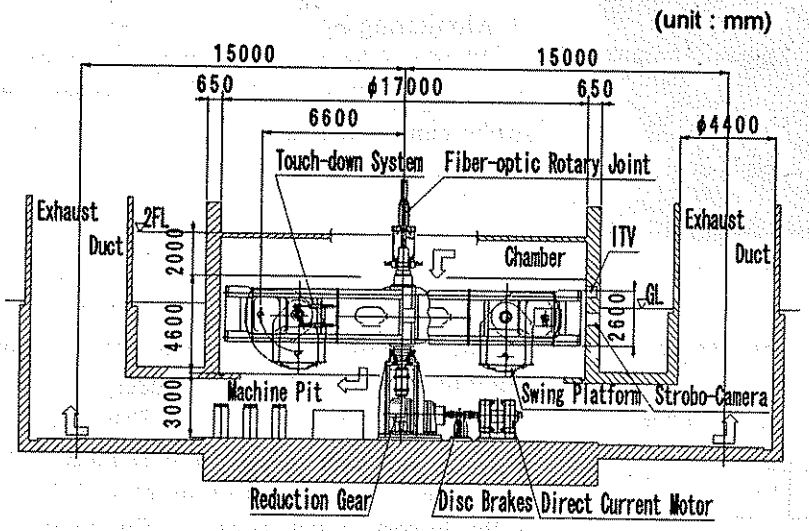

Fig.2 Schematic view of centrifuge

of the arm is lost and the horizontal displacement of the rotating axis measured with a gap sensor becomes large, the imbalance error signals are delivered and the weights are moved. The auto-balance capacity is 5 % of the maximum payload, that is 20G·ton.

3. DETA ACQUISITION AND MONITORING SYSTEM

(1) Rotary Joints

The centrifuge is equipped with rotary joints through which fluids can be sent to the platform. There are a total of 8 passages, with 6 rotary joints for oil and 2 rotary joints for either water or air.

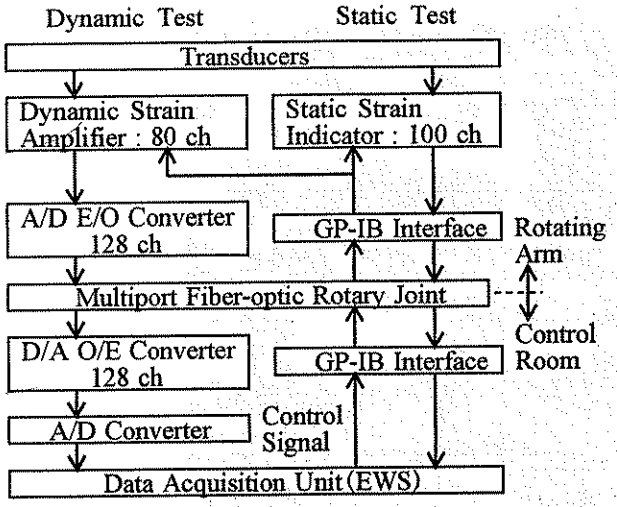

Fig.3 Flow of data acquisition

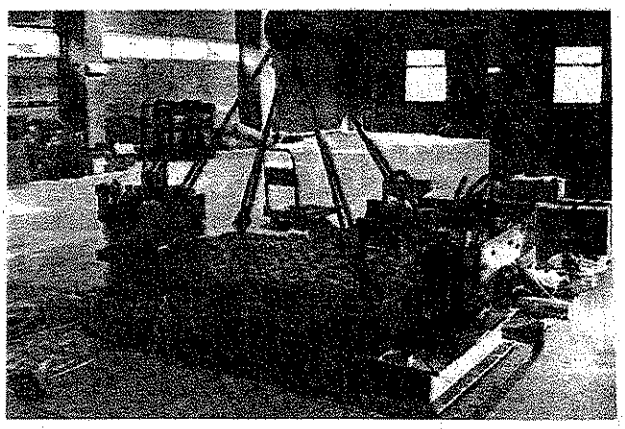

Fig.4 Photograph of Shaking table

Table 2 Specification of shaking table

Table Size	length : 1.7 m width : 1.0 m
Shaking Direction	horizontal : 1
Type of Shaking Wave	sinusoidal wave irregular wave
Maximum Centrifugal Acceleration	100 g
Maximum Shaking Acceleration	40 g
Maximum Velocity	90 cm/s
Maximum Displacement	±5 mm
Capacity	40 g-ton
Frequency Range	10 - 400 Hz

The capacity of working pressure is 10 MPa for oil and 0.7 MPa for water or air, respectively.

(2) Data Acquisition System

A diagram of the data acquisition system is shown in **Fig.3**. For dynamic tests, the analogue signals from transducers are amplified, digitized and converted into optical signals through the electro-optic converting unit mounted on the arm. Through the multiport fiber-optic rotary joint, the data are sent to the optic-electric converting unit in the control room and recorded on the internal disk of a workstation. For static tests, the signal outputs of transducers are recorded on the static strain indicator on the rotating arm. The data are sent to the workstation through the GP-IB interfaces. The dynamic strain amplifier and the static strain indicator are controlled from the workstation through the GP-IB interfaces.

(3) Monitoring System

Photographs and video images of a model on the swing platform in-flight can be taken with the strobo-camera and the CCD camera mounted on the arm, respectively.

4. SHAKING TABLE

(1) Specifications

An electro-hydrauric shaking table shown in **Fig.4** has been developed. Specifications of the shaking table are shown in **Table 2**. The capacity of the shaking table is as large as that of the shaker at UC Davis (Kutter et al. 1994) which is the largest in the world. The shaking table provides horizontal acceleration of 40G to a model of 1 ton. For the tests conducted at 50G, horizontal acceleration of 40G is equivalent to the maximum ground acceleration observed during the 1995 Hyogoken Nanbu earthquake.

(2) Earthquake Simulation System

The earthquake simulation system is composed of the excitation device, the hydraulic supply system, and the control system as shown in **Fig.5**.

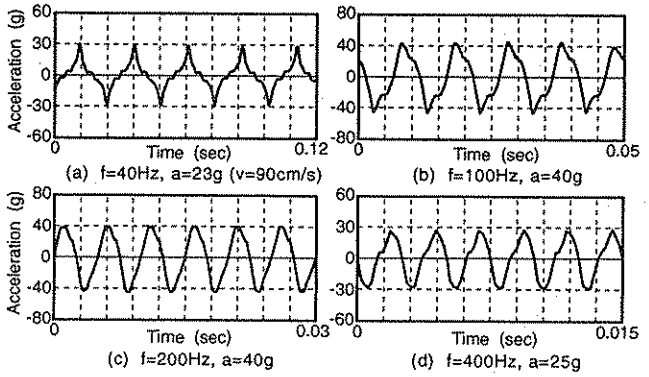

Fig.9 Recorded response acceleration-time history

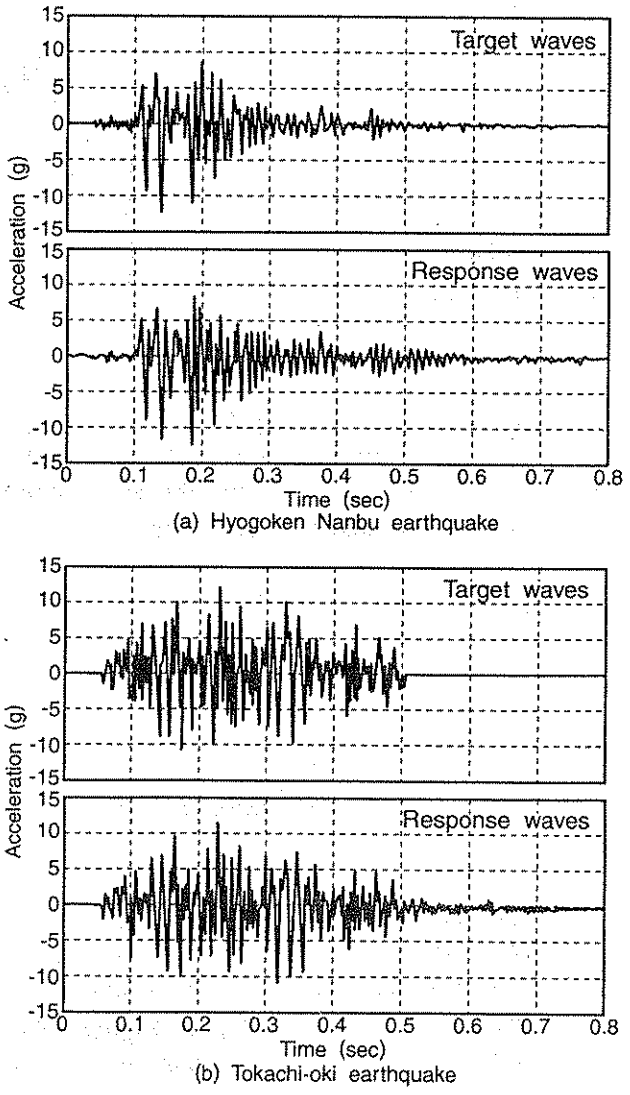

Fig.10 Comparison between target waves and response waves

extremely high frequency.

Next, two earthquake waves were used under 30G: the NS component of the Kobe Marine Observatory acceleration record in the 1995 Hyogoken Nanbu earthquake (Kobe wave), and the EW component of the Aomori Harbor acceleration record in the 1968 Tokachi-oki earthquake (Aomori wave). Each of the target waves was scaled so that the maximum acceleration was 12 g and the predominant frequency became 60 Hz. In **Fig.10** the response acceleration waves of the shaking table with a weight of about 1.4 ton are compared with the target earthquake waves. These input waves were corrected with the excitation control system. **Figure 11** shows that the response waves almost coincides with the target waves.

6. DYNAMIC CENTRIFUGE TEST

Several series of tests, aiming at investigating seismic behavior of huge bridge foundations on weak rock, retaining walls and embankment, and lateral spreading of liquefiable sand behind quay walls, were conducted in the centrifuge so far. Among them, results of tests on the retaining wall are briefly described in this section.

(1) Test procedures and conditions

In a rigid container with an internal dimensions of 150cm long×50cm deep×30cm wide, dry Toyoura sand was rained to form dense foundation soil of 10cm deep with relative density of approximately 80%. A model gravity retaining wall with a height of 30cm was placed on the foundation soil and the sand was rained again to build backfill behind the wall. The sand was rained intermittently so that accelerometers were set at the predetermined positions in the model. Configurations of various sensors in the model are shown in **Fig.11**. On the bottom and side of the model, a total of ten load cells which could measure normal and shear forces were built in.

Test conditions are summarized in **Table 3**. Relative density of the backfill was approximately

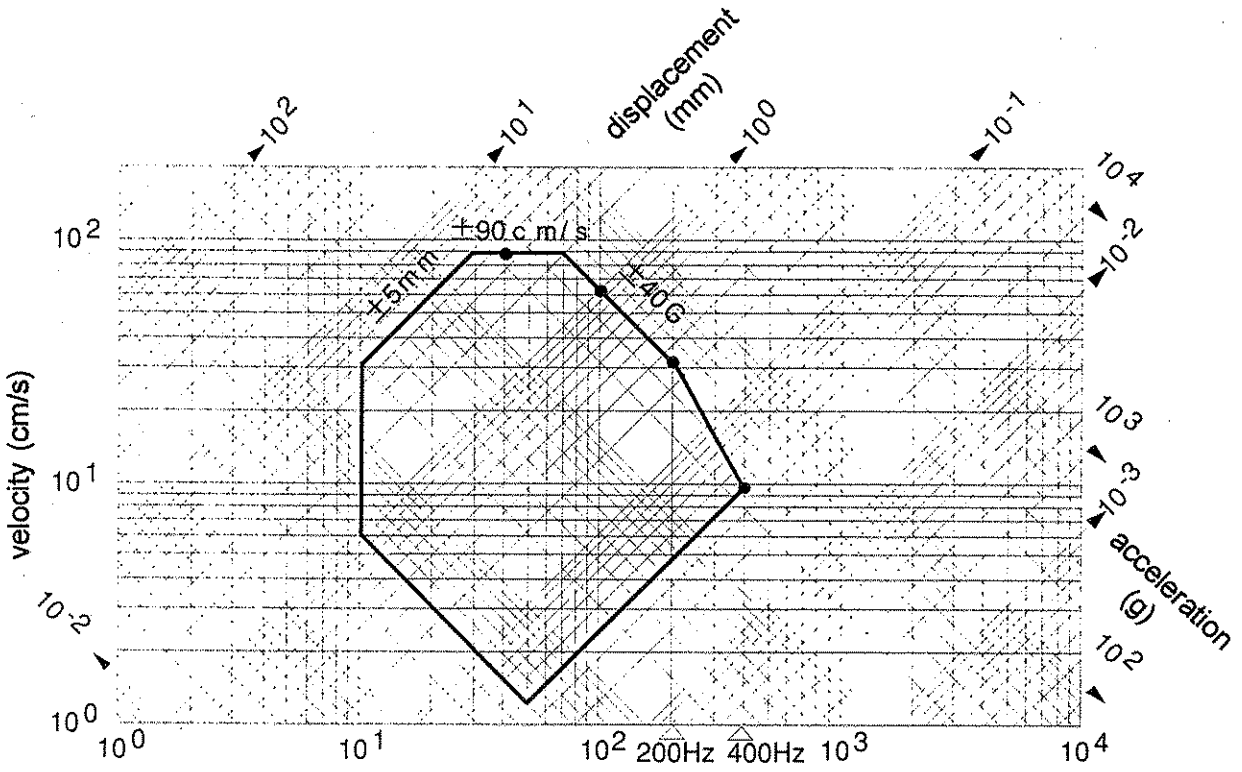

Fig.8 Shaking limit diagram

- The torque motor swings the armature according to the current.
- The pilot spool is driven up and down by the swing of armature.
- The quantity and the direction of oil supplied to a main spool are controlled by the movement of the pilot spool, and the main spool is driven right and left.
- The quantity and the direction of oil supplied to the actuator are controlled by the movement of the main spool, and the actuator is moved right and left.
- The excitation power is transmitted to the shaking table.

b) Hydraulic supply system

When dynamic tests are performed, it is necessary to supply a large amount of pressurized oil to the excitation device. Therefore, the oil is supplied continuously from the hydraulic pump in the machine pit to the accumulator on the rotation arm through the rotary joints.

c) Excitation control system

The excitation control system consists of the signal generation unit and the servo control unit. The control signal is transferred to the excitation device through the optical rotary joint. The signal generation device has the functions to generate input signal and to correct the input signal so as to adjust response waves to target waves according to the feedback signal from the excitation device.

5. PERFORMANCE

In order to check the performance of the shaking table, proof tests were carried out. At first, sinusoidal input acceleration was tested at 100G. Several points on the shaking limit line shown in **Fig.8** were selected. **Figure 9** shows the response acceleration time-histories of the shaking table with a model of some 400 kg fixed on it at frequencies of 40, 100, 200, 400 Hz. The figure indicates that response waves were distorted in the case of large displacement or

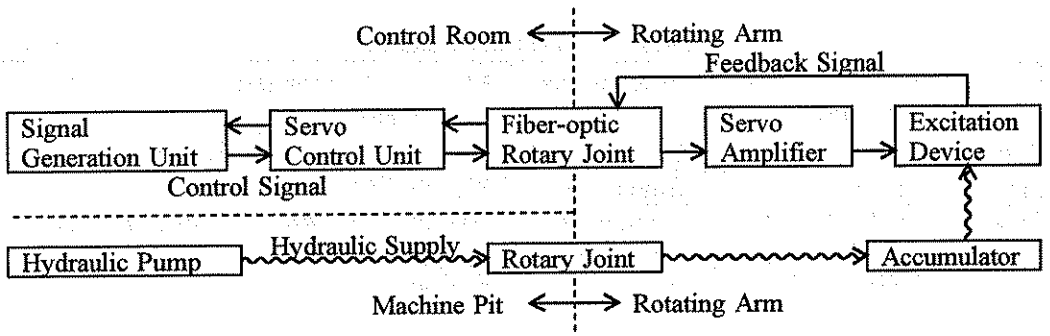

Fig.5 Earthquake simulation system

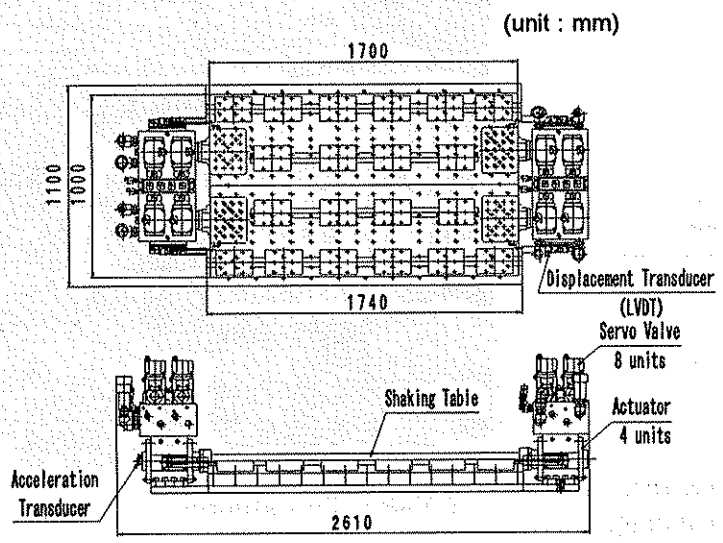

Fig.6 Plan and side view of shaking table

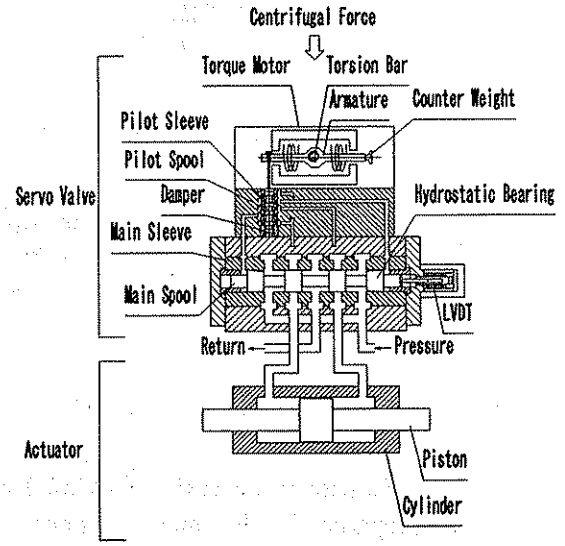

Fig.7 Schematic view of Actuator and servo valve

a) Excitation device

As shown in **Fig.6**, the excitation device is designed symmetrically. Two actuators which have two servo valves in each are arranged on both sides of the shaking table. In order to measure the displacement of actuators and the acceleration of shaking table for the control, LVDTs and accelerometers are put on the shaking table.

Figure 7 shows the structure of the actuator and the servo valve. The servo valve is composed of a large-scale torque motor, a pilot spool and a main spool, and controls the quantity and the direction of flowing oil to the actuator according to the movement of a main spool. In order to make the excitation capacity larger, it is necessary to supply a large quantity of flowing oil to the actuator. Therefore the diameter of the main spool become large, and the pilot spool is installed in order to drive the main spool hydraulically. The pilot spool hangs on the one end of armature in the direction of a centrifugal acceleration, and the counter weight is put on the opposite end. As a result, an unbalanced torque caused by the self-weight of the pilot spool and a friction torque by the vertical motion is deduced. The movement of the servo valve and the actuator is controlled along the following operation.

- The signal from the servo control unit is converted to the electric current by the servo amplifier, and the current is input to the torque motor.

Table 3 Test conditions

Test code	Relative density of backfill	Input motion	Max. acceleration tested (gals in prototype scale)	Centrifugal acceleration
Case1	82%	Sinusoidal	60, 95, 176, 288, 309, 353, 418	30G
Case2	61%	Sinusoidal	77, 198, 305, 450	
Case3	82%	Kobe wave	207, 262, 382, 481, 571, 600, 747, 823	
Case4	83%	Aomori wave	150, 173, 288, 358, 437, 498, 590	
Case5	83%	Sinusoidal	341, 424	

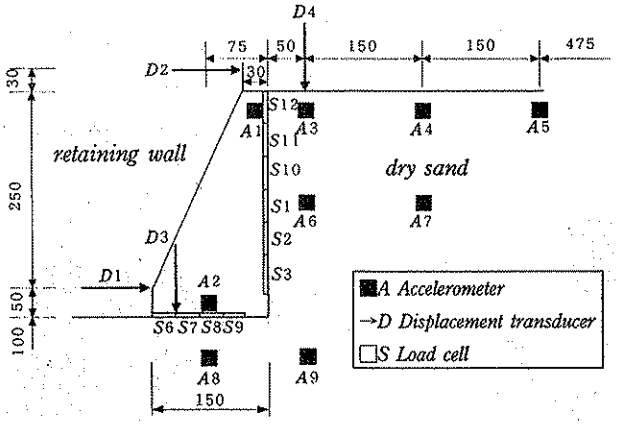

Fig.11 Model retaining wall

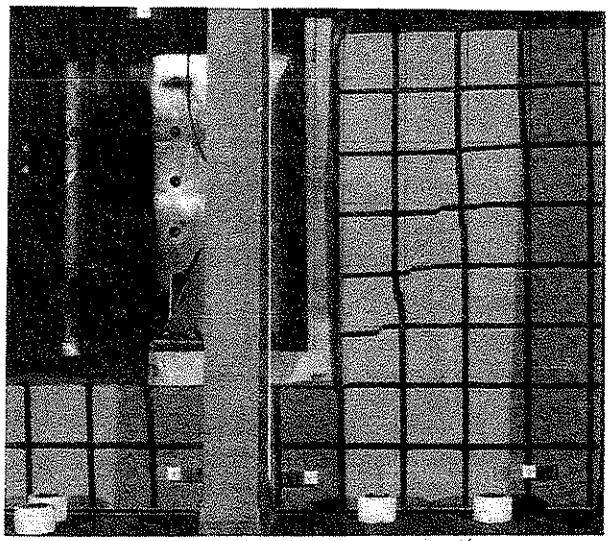

(a) after first shaking (341 gals)

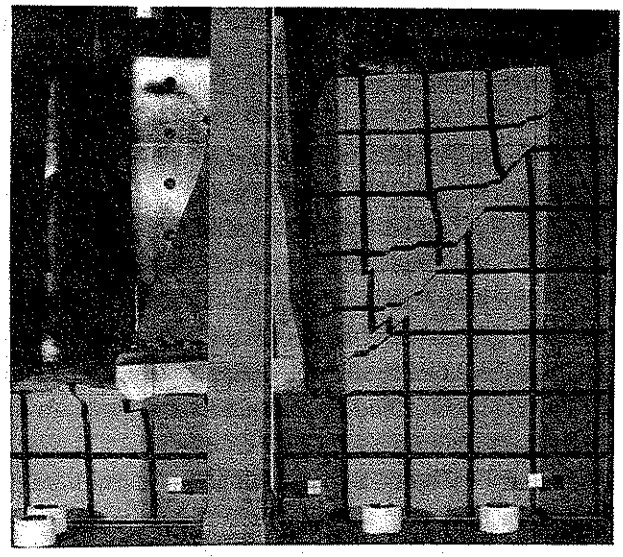

(b)after second shaking (424 gals)

Fig.12 Deformation of wall and backfill with clear slip surfaces (Case5)

80% with an exception for Case2 where sand was prepared in the medium dense condition(61% relative density). All the tests being carried out at 30G centrifugal acceleration field, the models are equivalent to prototype walls of 9m high. The models were excited horizontally with approximate sinusoidal wave with 30 uniform cycles of predominantly 60Hz acceleration for Case1, 2 and 5, Kobe wave for Case 3 and Aomori wave for Case 4. The time axis of the acceleration time histories of the two earthquake records were scaled so that predominant frequency becomes 60Hz. Shaking test was repeated several times for each model, with increased maximum acceleration α_m; for Case 1, for instance, 30 cycles of sine wave was applied for every step, with α_m= 1.99G (65 gals in prototype) for the first step, α_m=2.76G (90 gals) for second step, and so on.

(2) Results and discussions

In the following discussion, test results are

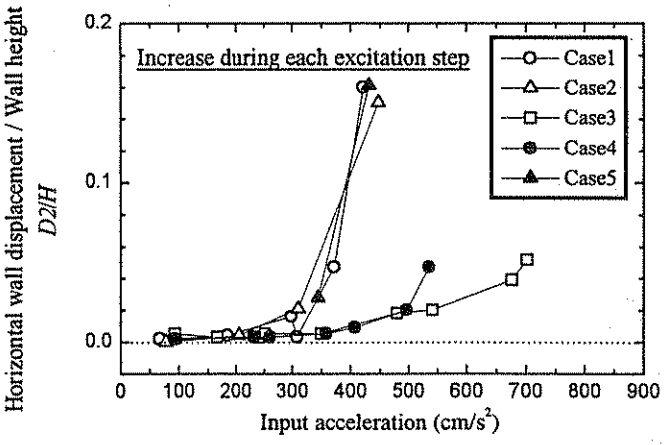

Fig.13 Variation of horizontal displacement increment versus input base acceleration

shown in the prototype sense otherwise mentioned; measured acceleration and frequency in the models are divided by a factor of 30. **Figure 12** shows photographs taken after shaking tests with α_m=341gals and 424gals in Case 5. It can be clearly seen in **Fig.12(a)** that the wall slid outwards and rotated counterclockwise and an active wedge with apparent slip surface developed in the back fill after shaking event of α_m=341 gals. The angle of the slip surface to the vertical agrees well with that predicted from well-known Mononobe-Okabe approach (Mononobe and Matsuo, 1929; Okabe, 1924) in conjunction with peak input acceleration and an angle of shearing resistance of the sand of 45 degree. After the shaking test with α_m=424 gals another slip surface with gentle slope was formed as shown in **Fig.12(b)**, as was predicted by Mononobe-Okabe approach.

Horizontal displacement increment of the top of the wall during each step divided by the wall height is plotted against α_m in **Fig.13**. For cases with sinusoidal wave, that is Case 1, 2 and 5, it was observed that there is a threshold acceleration of approximately 300gal below which displacement of the wall was less than 1% of the wall height and no slip surfaces developed during shaking. In the step with α_m higher than the threshold acceleration the model wall displaced largely and apparent slip surfaces were observed. This fact is consistent with results of a detail study by Bolton (1991) that active conditions are reached by outward movement of the order of 0.1% of the wall height in dense sand.

For Case 3 and 4, in which Kobe wave and Aomori wave were used, slip surfaces were observed after shaking step with α_m=571 gals and 498 gals respectively, and deformation of the walls did not largely increase in the subsequent step. This may be due to the fact that earthquake waves used in this study, in particular Kobe wave, had only several cycles of large acceleration, while 30 cycles of the maximum acceleration for the sinusoidal wave. It should be noted in **Fig.13** that displacement of the test with Aomori wave (Case 4) was larger than that with Kobe wave (Case 3). These observation confirms that many cycles with smaller peak acceleration contained in the real earthquake waves had little contribution to accumulate the deformation of the retaining walls.

The exact level of earthquake design of the retaining wall is uncertain, however, it is apparent that the threshold acceleration observed for Case 3 and 4, that is 571 gals and 498 gals respectively, was considerably in excess of any code requirement. This may indicate that displacement-based design approaches are needed.

The results presented in this section are part of ongoing project. Authors have been validating the Newmark's sliding block approach as a displacement based design method of retaining walls (Steedman, 1998) by comparing with test results.

REFERENCES

Kutter, B. L., Idriss, I.M., Khonke, T., Lakeland, J., Li, X.S., Sluis, W., Zeng, X., Tauscher, R.C., Goto, Y. and Kubodera, I. 1994. Design of a large earthquake simulator at UC Davis. Proc. Int. Conf. Centrifuge 94, Singapore. Balkema: 169-175.

Nagura, K., M. Tanaka, K. Kawasaki & Y. Higuchi 1994. Development of an earthquake simulator for the TAISEI centrifuge. Proc. Int. Conf. Centrifuge 94, Singapore. Balkema: 151-

156.
Mononobe N. and Matsuo H. 1929. On the determination of earth pressure during earthquakes, Proc World Engng. Congress, Vol.9, pp.177-185
Okabe S. 1924. General theory of earth pressure, Journal of Japan Civil Engng Society, Vol.12, No.1
Bolton M.D. 1991. Geotechnical stress analysis for bridge abutment design, Contractor report 270, Transport and Road Research Laboratory, Crowthorne, Berks.
Steedman R.S. 1998. Seismic design of retaining walls. Proc. Institution of Civil Engineers, Geotechnical Engineering, Vol.131, pp.12-22